



Power, M., Pomeroy, J., Anaya Calvo, J., Otoki, Y., Tanaka, T., Wada, J., Kuzuhara, M., Jantz, W., Souzis, A., & Kuball, M. (2014). Impact of buffer layers on thermal properties of AlGa_N/Ga_N-on-SiC high electron mobility transistors (HEMTs). In *Extended Abstracts of WOCSDICE-EXMATEC-2014, Delphi, Greece* (pp. 49-50)

Peer reviewed version

License (if available):
Unspecified

[Link to publication record in Explore Bristol Research](#)
PDF-document

University of Bristol - Explore Bristol Research

General rights

This document is made available in accordance with publisher policies. Please cite only the published version using the reference above. Full terms of use are available:
<http://www.bristol.ac.uk/red/research-policy/pure/user-guides/ebr-terms/>

Impact of buffer layers on thermal properties of AlGaN/GaN-on-SiC high electron mobility transistors (HEMTs)

M.Power^{1,*}, J.W. Pomeroy¹, J.Anaya Calvo¹, Y.Otoki², T.Tanaka², J.Wada², M. Kuzuhara³, W.Jantz⁴, A.Souzis⁵, M.Kuball¹

¹H.H. Wills Physics Laboratory, University of Bristol, Bristol BS8 1TL, UK

²Hitachi Metals, Ltd., Isagozawa 880, Hitachi City, Ibaraki 319-1418, Japan

³Department of Electrical and Electronics Engineering, University of Fukui, Japan

⁴SemiMap Scientific Instruments GmbH, Freiburg, Germany

⁵II-VI Wide Bandgap Group, Pine Brook, NJ 07058, USA

* E-mail: Maire.Power@bristol.ac.uk

ABSTRACT

In this work, a combination of Raman thermography and finite element thermal modelling was used to examine the thermal conductivities of different buffer layers in four AlGaN/GaN ungated high electron mobility transistors (HEMTs). The parameterisation of the thermal conductivities of iron-doped GaN, carbon-doped GaN and Al_{0.04}Ga_{0.96}N buffer layers gave good agreement in thermal simulations to experimentally-measured GaN temperatures obtained by Raman thermography. This shows the viability of the combined experimental and modelling method used in this work, for the extraction of layer thermal conductivities in complex AlGaN/GaN device heterostructures.

1. INTRODUCTION

AlGaN/GaN HEMTs are excellent candidates for high frequency[1] and high power applications[2]. During device operation, a temperature rise in the active GaN region of the device has a significant effect on device reliability and performance. There is therefore a need for effective heat extraction from this active region to the substrate heat sink. This thermal transport is affected by the thermal conductivity (κ) of the buffer layers and nucleation layer between the active region and substrate. Manoi *et al.*[3] have reported differences in active region temperature rises in AlGaN/GaN HEMTs with varying AlN nucleation layer quality and thickness. It is however also important to investigate the effect of different GaN buffer layer structures typically used in these devices on the heat extraction efficiency. There has been extensive research into the combination of experimental and thermal modelling to simulate temperature rises in the active region of AlGaN/GaN devices [4],[5]. These simulations can be used to examine the thermal conductivity of the layers between the active GaN device channel and the substrate in order to investigate thermal transport vertically through the AlGaN/GaN device. In this work, a combination of Raman thermography and finite element thermal modelling was used to investigate the thermal conductivities of different buffer layers in four AlGaN/GaN devices. This enabled the contribution of the different GaN buffer layers in the devices to vertical heat extraction efficiency to be compared.

2. EXPERIMENTAL

Four AlGaN/GaN ungated transistors with different vertical buffer layer structures as shown in Figure 1 were grown by metal organic chemical vapour deposition (MOCVD) on 370 μm thick vanadium-doped semi-insulating (SI) 6H-SiC substrates. The ungated transistors were surface-passivated with silicon nitride; for ohmic contacts Ti/Al/Mo/Au (15/60/35/50 nm) annealed at 850°C for 30 s in N₂ was used. Separations between contacts were between 4 and 20 μm , with a device width of 80 μm .

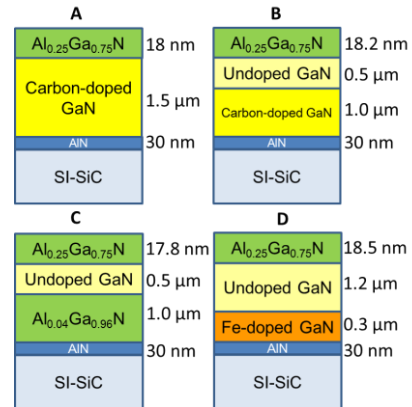


Figure 1: Heterostructure studies for four (A-D) AlGaN/GaN ungated HEMTs on SI-SiC substrates.

Raman thermography was utilized to measure the average temperature of the GaN layers in the devices using the temperature dependence of the GaN A₁(LO) phonon mode. The measurement was performed using a frequency-doubled Nd:YAG 532 nm CW laser of a Renishaw InVia spectrometer at a power of 3mW in which the ungated devices, placed on a copper heat sink, were mapped laterally by the laser beam from the middle of the active device region along the contacts to 60 μm outside the device. Device A, devices B and D and device C were operated with a power dissipation of 1.23W, 0.98W and 0.85W respectively. More details on the Raman thermography technique can be found in [6]. Three-dimensional (3D) finite element thermal modelling was performed for all the devices so as to simulate the device temperature; the average GaN lateral temperature was then compared to the experimental data recorded by

Raman thermography. By fitting of the temperature distribution of each device in the simulation to the experimental data the thermal conductivities of the GaN buffer layers were determined. The assumptions made in the model were that there was uniform power dissipation in the ungated devices and that the thermal conductivity, κ of the undoped and carbon-doped GaN layers were equal in the devices due to the carbon-doping concentration being less than the order of 10^{18} cm^{-3} [7]

3. RESULTS AND DISCUSSION

Figure 2 shows the average GaN, lateral temperature maps using Raman Thermography with the best fit, simulated temperature maps overlaid for devices A–D.

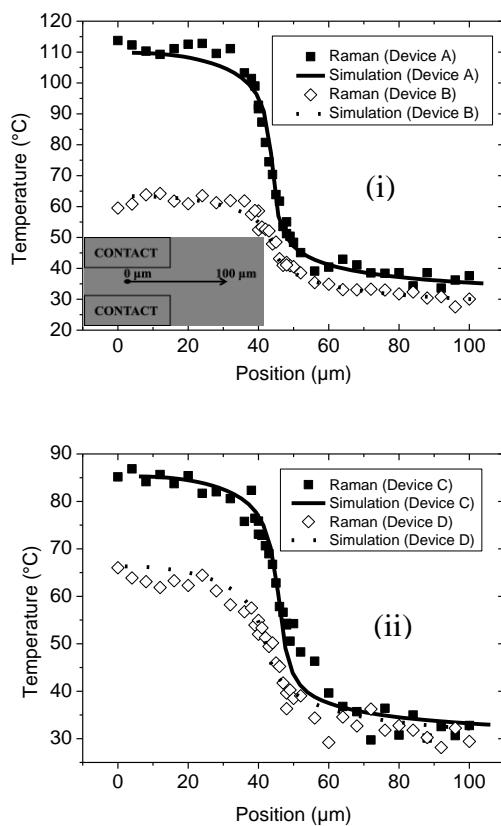


Figure 2: Experimentally-determined average GaN temperature measured from the centre of the devices to outside the active device region as indicated in the inset of (i), and simulated temperature fitted to the experimental data for (i) devices A and B with a contact separation of 4 μm and 20 μm respectively and (ii) devices C and D with a contact separation of 20 μm .

$\kappa(\text{SiC})$ was fixed at $400 \text{ W m}^{-1} \text{ K}^{-1}$ in all devices as a good fit of simulation to the experimental temperature map outside the device was obtained with this thermal conductivity value for device A. We note that outside the active device area, predominantly the substrate thermal conductivity impacts the GaN temperature, while inside the active device area, there are additional contributions from the GaN buffer layers and nucleation layer [8].

From the fitting of the simulated temperature profile to the experimental temperature map for device A, $\kappa(\text{carbon-doped GaN})$ and $\kappa(\text{AlN})$ were found to be 185

and $11 \text{ W m}^{-1} \text{ K}^{-1}$ respectively. κ of carbon-doped GaN reasonably matches previous literature values[4] and κ of the AlN layer suggests that the thermal boundary resistance associated with this layer is $2.8 \times 10^{-9} \text{ W}^{-1} \text{ m}^2 \text{ K}^{-1}$ which is on the lower end of previously reported values for AlN layers of similar thickness[3].

Using these parameters for the thermal model of device B with the assumption that carbon-doped GaN and undoped GaN have the same thermal conductivity gives a good fit of simulation to experimental results as seen in Figure 2(i), confirming the previously obtained thermal conductivity values for device A. Furthermore by using the same thermal conductivity values for undoped GaN and AlN in device C and D good fits were achieved with $\kappa(\text{Al}_{0.04}\text{Ga}_{0.96}\text{N})$ as $30 \text{ W m}^{-1} \text{ K}^{-1}$ which is in excellent agreement with previous literature values for $\text{Al}_x\text{Ga}_{1-x}\text{N}$ alloys[9] and $\kappa(\text{Fe-doped GaN})$ as $92 \text{ W m}^{-1} \text{ K}^{-1}$ which again agrees well with what can be expected considering point defect scattering and in comparison to the thermal conductivity of Si-doped GaN with a similar doping concentration [7]. It is important to note that because the iron-doped GaN layer is thin, the average GaN temperature is not as sensitive to the thermal conductivity of this layer so there is some uncertainty in determining this κ value.

4. CONCLUSION

The thermal conductivities of different GaN buffer layers in four AlGaN/GaN ungated device structures were investigated using a combination of Raman Thermography and a 3D finite element modelling approach. Thermal conductivities of $\text{Al}_{0.04}\text{Ga}_{0.96}\text{N}$, iron-doped GaN and carbon-doped GaN layers in the structures which match previous literature allowed for a good fit of simulation to experimental temperature data. This combined modelling and Raman thermography approach represents a viable way of examining the thermal conductivities of the individual layers of a group of complex AlGaN/GaN device structures.

5. REFERENCES

- [1] M. Kuzuhara, H. Miyamoto, Y. Ando, T. Inoue, Y. Okamoto, and T. Nakayama, *physica status solidi (a)*, 200, 167(2003)
- [2] M. Ishida, T. Ueda, T. Tanaka, and D. Ueda, *IEEE Trans. Electron Devices*, 60, 3053(2013)
- [3] A. Manoi, J. W. Pomeroy, N. Killat, and M. Kuball, *IEEE Electron Device Letters*, 31, 1395(2010)
- [4] A. Sarua, H. Ji, K. P. Hilton, D. J. Wallis, M. J. Uren, T. Martin, and M. Kuball, *IEEE Trans. Electron Devices*, 54, 3152(2007)
- [5] T. Batten, J. W. Pomeroy, M. J. Uren, T. Martin, and M. Kuball, *J. Appl. Phys.* 106, 94504(2009)
- [6] A. Sarua, H. Ji, M. Kuball, M. J. Uren, T. Martin, K. P. Hilton, and R. S. Balmer, *IEEE Trans. Electron Devices*, 53, 2438(2006)
- [7] J. Zou, D. Kotchetkov, A.A. Balandin, D.I. Florescu and F.H. Pollak, *J. Appl. Phys.* 92, 2534(2002)
- [8] J. W. Pomeroy, M. Bernardoni, D. C. Dumka, D. M. Fanning and M. Kuball, *Appl. Phys. Lett.* 104, 083513(2014)
- [9] S. Adachi, *J. Appl. Phys.* 102, 063502(2007)

